https://dx.doi.org/10.1016/j.atmosenv.2016.12.004 **This is the Pre-Published Version.**

Elsevier Editorial System(tm) for Atmospheric Environment

Manuscript Draft

Manuscript Number: ATMENV-D-16-00253R3

Title: Seasonal behavior of carbonyls and source characterization of formaldehyde (HCHO) in ambient air

Article Type: Research Paper

Keywords: carbonyl; seasonal variation; source apportionment analysis; ambient air; correlation analysis.

Corresponding Author: Dr. Kin Fai Ho,

Corresponding Author's Institution: The Chinese University of Hong Kong

First Author: Ka Hei Lui

Order of Authors: Ka Hei Lui; Steven Sai Hang Ho; Peter K. K. Louie; C. S. Chan; S. C. Lee; Di Hu; P. W. Chan; Jeffrey Chi Wai Lee; Kin Fai Ho

Abstract: Gas-phase formaldehyde (HCHO) is an intermediate and a sensitive indicator for volatile organic compounds (VOCs) oxidation, which drives tropospheric ozone production. Effective photochemical pollution control strategies demand a thorough understanding of photochemical oxidation precursors, making differentiation between sources of primary and secondary generated HCHO inevitable. Spatial and seasonal variations of airborne carbonyls based on two years of measurements (2012-2013), coupled with a correlation-based HCHO source apportionment analysis, were determined for three sampling locations in Hong Kong (denoted HT, TC, and YL). Formaldehyde and acetaldehyde were the two most abundant compounds of the total quantified carbonyls. Pearson's correlation analysis ($r > 0.7$) implies that formaldehyde and acetaldehyde possibly share similar sources. The total carbonyl concentration trends (HT < TC < YL) reflect location characteristics (urban > rural). A regression analysis further quantifies the relative primary HCHO source contributions at HT (~13%), TC (~21%), and YL (~40%), showing more direct vehicular emissions in urban than rural areas. Relative secondary source contributions at YL (~36%) and TC (~31%) resemble each other, implying similar urban source contributions. Relative background source contributions at TC could be due to a closed structure microenvironment that favors the trapping of HCHO. Comparable seasonal differences are observed at all stations. The results of this study will aid in the development of a new regional ozone (O3) control policy, as ambient HCHO can enhance O3 production and also be produced from atmospheric VOCs oxidation (secondary HCHO).

© 2016. This manuscript version is made available under the CC-BY-NC-ND 4.0 license http://creativecommons.org/licenses/by-nc-nd/4.0/

Highlights:

- Formaldehyde (HCHO) and acetaldehyde together contribute >70% to total carbonyls
- Strong correlation between the two compounds implies same source
- Rural area with low vehicular emissions shows lowest primary HCHO contribution
- Highest primary source signal in winter due to direct emissions at low temperature
- Acetone not reported due to DNPH cartridge shows negative biases in measurement

*Manuscript
Click here to download Manuscript: C_AE_3_U_F1.docx Click here to view linked References

Seasonal behavior of carbonyls and source characterization of formaldehyde (HCHO) in ambient air

K. H. Lui[a], Steven Sai Hang Ho[b,c], Peter K. K. Louie[d], C. S. Chan[a], S. C. Lee[e], Di Hu[f], P. W. Chan[g], Jeffrey Chi Wai Lee[g] , K. F. Ho[a,b*]

[a]*The Jockey Club School of Public Health and Primary Care, The Chinese University of Hong Kong, Hong Kong, China*

[b]*Key Laboratory of Aerosol Chemistry and Physics, SKLLQG, Institute of Earth Environment, Chinese Academy of Sciences, Xi'an, 710075, China*

[c]*Division of Atmospheric Sciences, Desert Research Institute, Reno, NV89512, USA*

[d]*Hong Kong Environmental Protection Department, 33/F., Revenue Tower, 5 Gloucester Road, Wan Chai, Hong Kong*

[e]*Department of Civil and Structural Engineering, Research Center of Urban Environmental Technology and Management, The Hong Kong Polytechnic University, China*

[f]*Department of Chemistry, Hong Kong Baptist University, Kowloon Tong, Kowloon, Hong Kong, China*

[g]*Hong Kong Observatory, 134A Nathan Road, Kowloon, Hong Kong*

[*]Corresponding author. Tel.: +852 22528763; fax: +852 26063500

E-mail address: kfho@cuhk.edu.hk

Abstract

Gas-phase formaldehyde (HCHO) is an intermediate and a sensitive indicator for volatile organic compounds (VOCs) oxidation, which drives tropospheric ozone production. Effective photochemical pollution control strategies demand a thorough understanding of photochemical oxidation precursors, making differentiation between sources of primary and secondary generated HCHO inevitable. Spatial and seasonal variations of airborne carbonyls based on two years of measurements (2012–2013), coupled with a correlation-based HCHO source apportionment analysis, were determined for three sampling locations in Hong Kong (denoted HT, TC, and YL). Formaldehyde and acetaldehyde were the two most abundant compounds of the total quantified carbonyls. Pearson's correlation analysis ($r > 0.7$) implies that formaldehyde and acetaldehyde possibly share similar sources. The total carbonyl concentration trends (HT < TC < YL) reflect location characteristics (urban > rural). A regression analysis further quantifies the relative primary HCHO source contributions at HT (~13%), TC (~21%), and YL (~40%), showing more direct vehicular emissions in urban than rural areas. Relative secondary source contributions at YL (~36%) and TC (~31%) resemble each other, implying similar urban source contributions. Relative background source contributions at TC could be due to a closed structure microenvironment that favors the trapping of HCHO. Comparable seasonal differences are observed at all stations. The results of this study will aid in the development of a new regional ozone (O_3) control policy, as ambient HCHO can enhance O_3 production and also be produced from atmospheric VOCs oxidation (secondary HCHO).

Keywords:

Carbonyl, Seasonal Variation, Source Apportionment Analysis, Ambient Air, Correlation Analysis

1. Introduction

Over the past three decades, environmental scientists worldwide have paid much attention to airborne carbonyls (aldehydes and ketones) in urban air. Carbonyls such as formaldehyde (HCHO) and acetaldehyde (CH_3CHO) are key components in photochemical reactions that cause air pollution (Anderson et al., 1996). Sources of carbonyls are generally classified as either natural or anthropogenic, and the carbonyls from these sources are defined as primary (direct emissions) or secondary (formed in the atmosphere). Examples of carbonyl sources are incomplete combustion of fossil fuels and biomass, industrial emissions, vehicular exhaust, and photochemical oxidation of atmospheric hydrocarbons (Atkinson, 2000; Carlier et al., 1986; Grosjean et al., 2002; Kean et al., 2001; Lee et al., 1997; Perry and Gee, 1995; Yokelson et al., 1999). The lifetime of formaldehyde, in the sunlit troposphere, does not exceed four hours (De Smedt et al., 2008; Wert et al., 2003), depending on different physicochemical properties and production/removal pathways (DeMore, 1992). Formaldehyde has a short daytime lifetime and is removed mainly from the atmosphere via photolysis. HCHO photolysis can cause perhydroxyl radicals (HO_2) formation, which react with nitrous oxide (NO) rapidly converting to hydroxyl radicals (OH) (Garcia et al., 2006). These processes drive photo-oxidation and ultimately lead to ozone (O_3) formation, which is an ambient air pollution species in urban areas (Parrish et al., 2012).

Hong Kong (22°16′1.2″N, 114°11′16.8″E) is a region on the southern coast of China, geographically enclosed by the Pearl River Delta (PRD) and the South China Sea. Only ~15% is urban, and the average population density reaches 6544 persons per km^2 (Census and Statistics Department, 2012). The number of registered private cars reached 501,021 in March 2013 (Hong Kong Transportation Department, 2013). Such high population density and number of vehicles invariably contribute to high ambient carbonyl concentrations (Ho et

al., 2006). Motor vehicle emission is one of the primary emission sources of formaldehyde (Anderson et al., 1996). Formaldehyde from direct emissions could accumulate at night and initiate photochemical reactions in the diurnal cycle during the day (Parrish et al., 2012). The quantification of primary and secondary sources of formaldehyde in Hong Kong is important, as these emission sources can be used to target urban O_3 concentration reduction.

The present study explores the characteristics of airborne carbonyls in different areas of Hong Kong, in addition to further quantifying the aforementioned sources by regression analysis. This aims to progress further than a recent study conducted by Cheng et al. (2014). The outcome is an important preliminary step for setting up future control policies and regulations for the city.

The aim of this study is to: 1) investigate the spatial variations of carbonyls in ambient air; 2) identify correlations between the spatial variations and meteorological conditions; 3) quantify the relative contributions of primary and secondary formaldehyde sources in order to develop an effective urban ozone control policy.

2. Materials and methods

2.1. Sampling locations and meteorological conditions

The Environmental Protection Department (HKEPD) is a department of the Hong Kong Government concerning the issues of environmental protection in Hong Kong. The HKEPD has been conducting regular citywide airborne carbonyl sampling in Hong Kong with the goal of identifying and tackling air pollution. Three Air Quality Stations located at Hok Tsui (HT) (22^o 12' 18.0"N, 114^o 15' 36.0"E), Tung Chung (TC) (22^o 17' 20.0"N, 113^o 56' 37.0"E), and Yuen Long (YL) (22^o 26' 43.0"N, 114^o 1' 22.0"E) (Fig. 1) were selected for air sample

collection. The sampling locations are fixed monitoring stations under the air quality monitoring network operated by the HKEPD, which represent both rural (HT) and urban areas (TC and YL).

Hok Tsui station is located at the end of Cape D'Aguilar Road at the southeastern tip of Hong Kong Island, adjacent to the South China Sea. The sampling station is in a remote area and far removed from any anthropogenic activities, ~2.5 km away from major traffic (Shek O Road). The carbonyl sampler was installed in a large shelter which was equipped with air conditioner, with the sampling inlet ~4 m above the ground level outside the shelter. Tung Chung station is located on the northwestern coast of Lantau Island and surrounded by a residential area. The air sampler is located on the rooftop of a four-floor building, ~16 m above the ground level, in proximity of the heavily used North Lantau Highway (~60 m away). Yuen Long station is situated on the Yuen Long Plain. Yuen Long (location YL) is a town with a population of 587,800 in 2013 (Social Welfare Department, 2013). The air sampler is located in the central Long Ping area on the rooftop of a six-floor building, ~28 m above the ground level and ~70 m away from major traffic (Castle Peak Road). Yuen Long station is located closer to continental China than Tung Chung station.

Hong Kong is characterized by a subtropical climate dominated by the East Asian monsoon. Prevailing winds are north/northeast during winter, east during spring and autumn, and south/southwest during summer.

2.2. Sample collection

Sample collection was integrated over a 24-hour interval (beginning at 00:00 UTC+8) and samples were collected during all four seasons from 2012 to 2013. Seasons were defined as follows: winter (01 December–28 February); spring (01 March–31 May); summer (01 June–

31 August); autumn (01 September–30 November). Sampling was carried out during the period between 4 and 14 days each month, and a total of 151 (HT), 151 (TC), and 153 (YL) samples were collected between 2012 and 2013. The air samples were collected in silica cartridges impregnated with acidified 2,4-dinitrophenylhydrazine (DNPH) (Sep-Pak DNPH-silica, 55–105 μm particle size, 125 Å pore size; Waters Corporation, Milford, MA) at a flow rate of 0.7 L min^{-1} using an ATEC 8000 cartridge sampler. Collection efficiencies were confirmed in the field by sampling carbonyls in two identical cartridges connected in series. Efficiencies were calculated as 100% ($1-A_b/A_f$), in which A_f and A_b denote the amount of carbonyls collected in the front and back sampling tubes, respectively. No breakthrough was observed in the sampling flow rate and time used. The sampling flow rates were checked in the field at the start and end of each sampling period using a calibrated flow meter (Gilibrator Calibrator; Gilian Instruments, W. Caldwell, NJ). A Teflon filter assembly (Whatman, Clifton, NJ) and ozone scrubber were connected to the front of the DNPH-silica cartridge to remove any particulate matter and prevent possible contamination by ozone (Spaulding et al., 1999). Collocated samples were collected to test sample collection reproducibility (>95%) in the field. A cartridge was reserved for field blank analysis during each sampling campaign and was handled in the same manner as the other sampling cartridges. The amount of carbonyls detected in the cartridges was corrected for the field blank before conversion to air concentration of carbonyl units. The DNPH-coated cartridges were stored in a refrigerator (<4°C) prior to analysis.

2.3. Carbonyl analysis

A total of 15 carbonyls were quantified, including formaldehyde (C1), acetaldehyde (C2), acrolein (ACRO), propionaldehyde (nC3), crotonaldehyde (CROT), methyl ethyl ketone (MEK), butyraldehyde/isobutyraldehyde (iso+nC4), benzaldehyde (benz), isovaleraldehyde

(iso-C5), valeraldehyde (nC5), *o*-tolualdehyde (o-tol), *m*-tolualdehyde (m-tol), *p*-tolualdehyde (p-tol), hexaldehyde (C6), and 2,5-dimethylbenzaldehyde (2,5-DB). Unsaturated carbonyls such as acrolein and crotonaldehyde were detected but not reported because of their low abundances. The sampling campaign determined carbonyl compounds in ambient air following the U.S. Environmental Protection Agency (EPA) Method TO-11A (USEPA, 1999). This method is not appropriate for the hydroxyl carbonyls (e.g. glycolaldehyde and hydroxyacetone) and dicarbonyls (e.g. glyoxal) analysis. Acetone was not analyzed due to biases associated with carbonyl measurement using active air sampling through a 2,4dinitrophenylhydrazine (DNPH)-coated solid sorbent cartridge following the currently used U.S. EPA Method TO-11A in this study (USEPA, 1999). The method shows negative biases for the determination of unsaturated aldehydes. Unsaturated carbonyl DNP-hydrazones can react with excess reagent to form adducts, leading to ambiguities in quantification due to chromatographic interferences (e.g., double peaks) and response factor issues (Ho et al., 2011; Schulte-Ladbeck et al., 2001). In addition, acetone is less reactive than aldehydes in the derivatization with DNPH, resulting in poor collection efficiency (Ho et al., 2014). In-house laboratory experiments demonstrated that collection efficiencies were >93±5% for all target carbonyls under the same flow rate, relative humidity, and temperature. Another ketone of MEK had an acceptable collection efficiency of >80% under the sampling environment. Collection efficiencies for heavy carbonyl compounds (e.g., C6) were recorded to be >96±3%. Each DNPH-coated cartridge was eluted with 2.0 mL acetone-free acetonitrile solution (HPLC/GCMS grade, J&K Scientific Ltd., Ontario, Canada) and transferred to a volumetric flask. Previous studies demonstrated that neither DNPH nor DNPH derivatives remained in the cartridge after elution with 2.0 mL acetone-free acetonitrile solution (Ho et al., 2007). Certified calibration standards for monocarbonyl DNP-hydrazones were purchased from Supelco (Bellefonte, PA) and diluted to a concentration range of 15–3000 μg mL^{-1}. The

calibration solutions were allowed to rest at room temperature for six hours for complete derivatization. The final volume of each calibration solution was filled up to 2.0 mL with acetonitrile/pyridine (HPLC/GCMS grade, Sigma) at a concentration ratio of 8:2 (v/v). The calibration curve was linearized, and the correlation of determination (r^2) was >0.999. The calibration standards and cartridge extracts were analyzed by injecting 20 μL of the solution into a high-pressure liquid chromatography (HPLC) system (Series 1200; Agilent Technology, Santa Clara, CA) coupled with a photodiode array detector (DAD). A reversed-phase separation column (4.6 × 250 mm Spheri-5 ODS 5 μm C-18, PerkinElmer, Norwalk, CT) was installed in the HPLC system and operated at room temperature (25°C). The mobile phase consisted of three solvent mixtures: mixture A, 6:3:1 (v/v) of water/acetonitrile/tetrahydrofuran; mixture B, 4:6 (v/v) of water/acetonitrile; and mixture C, acetonitrile. The gradient program was operated first at (80% A)/(20% B) for one minute, second at a linear gradient of (50% A)/(50% B) for eight minutes, third at (100% B) for ten minutes, fourth (100% C) for six minutes, and finally at (100% C) for five minutes. The elution rate was 2.0 mL min^{-1}. The absorbance of the 360 and 390 nm wavelengths was applied to identify aliphatic and aromatic carbonyls (e.g., benzaldehyde and tolualdehyde), respectively. Identification and quantification of carbonyl compounds were based on retention time and peak area integration of different carbonyl compounds. The minimum detection limit (MDL) was estimated by analyzing a minimum of seven replicates of standard solution containing analyte at a concentration of 0.015 μg mL^{-1}. The following equation was used to estimate the MDL:

$$MDL = t_{(n-1,1-\infty=99\%)} \times s \quad (1)$$

where $t_{(n\text{-}1,1-\infty\,=\,99\%)}$ is the student's t-distribution value at n-1 degrees of freedom and *S* is the standard deviation of the replicates. The MDLs of the target carbonyls range from 0.002 to 0.010 ng μL^{-1}, which can be translated to 0.016–0.12 ppbv at a sampling volume of 2.02 m^3.

Measured values, precision, accuracy, and validity were optimized throughout the measurements. Quality assurance was performed to ensure the above attributes were within acceptable limits. A quality control procedure was included to assure a measurement precision of 0.5–3.2% for the measured carbonyls. Further details of the collection efficiency and quality control procedures can be found in Text S1-2 (Supplementary Material).

2.4. Statistical and planetary boundary layer condition analysis

Pearson's correlation coefficient analysis was used to test correlations between all analyzed carbonyl compounds and meteorological parameters. The meteorological parameters were collected by the Hong Kong Observatory (HKO). All data were analyzed using SPSS statistic 21.0 (IBM®, New York, NY) or GraphPad Prism software (Version 5 for Windows).

The boundary layer condition in 2012-13 at Hong Kong (Latitude: from 22^{o} 11' 34.428" to 22^{o} 27' 0.252"; Longitude: from 113^{o} 55' 17.651" to 114^{o} 16' 0.012" was collected from The European Centre for Medium-Range Weather Forecasts (ECMWF) (Dee et al., 2012). The boundary condition of the model assimilated dynamical inputs (0.125^{o} x0.125^{o}) in every 3-hour interval for 24-hour daily during 2012-2013.

2.5. Source characterization for formaldehyde

Correlation-based source apportionment analysis was used to distinguish between primary emissions and secondary formation processes of formaldehyde. A tracer approach was applied using collocated daily ambient concentrations of carbon monoxide (CO) and ozone (O_3) as tracer species to identify primary and secondary sources of formaldehyde. Relative contributions of different sources of formaldehyde were estimated by statistical analysis (Friedfeld et al., 2002; Garcia et al., 2006; Li et al., 2010). The equation for the linear

regression model used is shown below:

$$[HCHO] = b_0 + b_1[O_3] + b_2[CO] \quad (2)$$

where b_0, b_1, and b_2 are the coefficients of the linear regression model. The equation is defined so that for every unit increase in O_3 concentration, there is a b_1 unit increase in *HCHO* concentration; for every unit increase in *CO* concentration, there is a b_2 unit increase in *HCHO* concentration; b_0 represents the background *HCHO* concentration that can neither be classified as primary nor secondary in the linear regression model. The background *HCHO* concentration may change, and hence introduce a bias to the *b*-values in Eq. (2) (Garcia et al., 2006). All concentration units are in μg m^{-3}. Relative contributions from emissions, photochemical reactions, and background *HCHO* concentrations can be computed according to the tracer concentrations and corresponding *b*-values by the following equations:

$$R_s = \frac{\sum(b_1[O_3]_t)}{\sum(b_0 + b_1[O_3]_t + b_2[CO]_t)} \times 100\% \quad (3)$$

$$R_p = \frac{\sum(b_2[CO]_t)}{\sum(b_0 + b_1[O_3]_t + b_2[CO]_t)} \times 100\% \quad (4)$$

$$R_B = \frac{b_0}{\sum(b_0 + b_1[O_3]_t + b_2[CO]_t)} \times 100\% \quad (5)$$

where R_S denotes the relative percentage contribution of *HCHO* from secondary sources, R_P denotes the relative percentage contribution of *HCHO* from primary sources, and R_B denotes the relative percentage contribution of *HCHO* that is neither from primary nor secondary sources. Background contributions (R_B) of *HCHO* may be due to alternate *HCHO* sources with different residence times or the transport of *HCHO* into the airshed, which may introduce a bias to the *b*-values in Eq. (2). The symbols $[CO]_t$ and $[O_3]_t$ denote concentrations of *CO* and O_3 at time *t*, and b_0, b_1, and, b_2 are the coefficients of the linear regression model (Eq. 2). Statistical analysis using carbon monoxide and glyoxal (CHOCHO) as tracers for formaldehyde source analysis, as described by Garcia et al. (2006), was impossible because

of unavailable time series data for CHOCHO. However, the advantage of using CHOCHO over O_3 is that CHOCHO has similar sink terms to HCHO, in contrast to O_3, resulting in a similar atmospheric lifetime, while being a good indicator of secondary formaldehyde as CHOCHO is mainly secondary in origin with similar sources as secondary HCHO, i.e., VOC oxidation (Garcia et al., 2006). Therefore, using the current CO-O_3 tracer pair could have limitation towards the outcome of the analysis.

3. Results and discussion

3.1. Ambient concentrations of carbonyls

The concentrations of individual carbonyls and the tracers at each sampling location are summarized in Table 1 and Supplementary Materials: Table S1, respectively. The time series plot of the carbonyl concentrations and corresponding meteorological conditions during the sampling period can be found in Supplementary Materials: Figure S1-3. The formaldehyde, acetaldehyde, carbon monoxide, ozone, and temperature data represent continuous time series measured at regular intervals. The time series data is used to demonstrate serial correlation without relying on statistical tests that assume independence among observations. The results of time series plots are consistent with the highest formaldehyde concentrations in autumn in urban southern California found in a previous study (Grosjean, 1991).

The average total concentrations of carbonyls at HT, TC, and YL sampling locations in 2012 were 4.2 ± 1.2 μg m^{-3}, 8.8 ± 1.8 μg m^{-3}, and 9.4 ± 1.3 μg m^{-3}, respectively. In addition, in 2013, the average total concentrations at HT, TC, and YL were 4.3 ± 0.6 μg m^{-3}, 9.0 ± 1.4 μg m^{-3}, and 10.6 ± 2.0 μg m^{-3}, respectively. These results correspond to the location characteristics of the sampling sites as discussed in Section 2.1. Both TC and YL are

characterized by substantial anthropogenic activities and indeed show different total carbonyl concentrations than HT. With good ventilation and little anthropogenic interference, results for HT reflect the natural carbonyl concentrations in this rural location. Average yearly total carbonyl concentrations are comparable to another study (Cheng et al., 2014). Cheng et al. (2014) showed that the sum of carbonyl compounds in roadside, urban, and background areas of Hong Kong was 12.2 ± 3.5 μg m^{-3}, 10.5 ± 4.8 μg m^{-3}, and 5.1 ± 3.4 μg m^{-3}, respectively, during 2011–2012. The present results are consistent with other sampling locations in the city, and also comparable to concentration ranges in neighboring Guangzhou City (Feng et al., 2005) and at the border of Cabañeros National Park, Spain (Villanueva et al., 2014). The results from HT show even lower total carbonyl concentrations than the predetermined background station reported in Cheng et al.'s (2014) study. The formaldehyde concentrations at HT, TC, and YL are in the range of 2.4 ± 0.5 to 5.2 ± 1.0 μg m^{-3} and it is the most abundant compound. Concentrations for the next most abundant carbonyl compound (acetaldehyde) range from 1.0 ± 0.3 to 2.8 ± 0.6 μg m^{-3}. Acetone was not analyzed due to negative biases for the determination of unsaturated aldehydes and ketones (acetone) and poor collection efficiency in the U.S. EPA Method TO-11A (USEPA, 1999; Ho et al., 2014). A previous study showed concentration of acetone was in a range of 1.14-1.43 μg m^{-3} at different air monitoring stations in Hong Kong (Ho et al., 2002b). The overall concentration profiles show trends similar to those seen in other studies (Cheng et al., 2014; Ho et al., 2002a), with formaldehyde and acetaldehyde as the two most abundant components. The C_1/C_2 ratios were also determined and listed with other studies (Supplementary Materials: Table S2).

3.2. Seasonal variations

Table 1 lists the average seasonal concentrations of carbonyls for 2012–2013. The corresponding meteorological parameters are shown in Table 2. In autumn, the highest formaldehyde and acetaldehyde concentrations, along with the highest ozone concentrations, were measured at all locations (Supplementary Materials: Figure S1-3). The high concentrations could be due to photochemical reactions of volatile organic compounds (VOCs) and also lead to production of ozone. An increase in average wind speed, coupled with prevalent easterly to northeasterly winds was also observed during autumn (Supplementary Materials: Figure S4-5). This observation points to possibly a transfer of aged and contaminated air masses (in this case, with formaldehyde and acetaldehyde) to Hong Kong. Biomass burning in China could be related to elevated concentrations of formaldehyde and acetaldehyde, although further investigation is required (Streets et al., 2003). A monthly climatology of mean planetary boundary layer heights (PBL) in 2012-2013 is shown in Supplementary Materials: Figure S6. The result is consistent with a long-term (~6.5 years) Lidar measurement in Hong Kong. The study showed mixing layer height is highest in autumn instead of summer. This could be due to higher relative humidity in summer than autumn, which favored larger amount of low-level cloud formation (Yang et al., 2013). Mixed layer depths reflect boundary layer turbulence and volume related to surface-emitted pollutants (Stull, 2012). The average boundary layer height is shallowest in spring (392.8 ± 36.7 m), however deepest in autumn (651.5 ± 108.3 m). Further studies on the relationships between PBL height and concentration of carbonyl compounds are required in future analysis. Other carbonyls show no clear seasonal variation, although slight concentration fluctuations among seasons are noticeable during the sampling period. Inconsistent seasonal variations of carbonyl compounds were observed in this study, which are on par with previous studies elsewhere in Hong Kong and worldwide (Ho et al., 2002b; Moussa et al., 2006).

Among the three stations, HT is usually the first station to experience clean marine air masses from the South China Sea or the North Pacific Ocean under prevailing southerly or southeasterly winds. Different site geographical locations could lead to different observed seasonal concentrations. All summer to winter ratios, except that of isovaleraldehyde, were <1 at HT and YL in 2013. However, mixed summer to winter ratios is shown in TC. The average total quantified carbonyl concentration at HT is, in descending order: autumn > winter > spring > summer. At TC, the trend is, in descending order: autumn > summer > winter > spring, and in YL the order is autumn > winter > spring > summer. The autumn season is characterized by moderate temperatures, light northeasterly winds, and little precipitation. Light winds could promote transport of polluted air from Asia to Hong Kong, in addition to an accumulation of locally emitted carbonyls. The lowest average total carbonyl concentrations at HT during the summer could be due to prevailing southerly or southeasterly winds (Supplementary Materials: Figure S4-S5) drawing clean marine air masses from the South China Sea or the Northwest Pacific Ocean, diluting total carbonyl concentrations. All locations show higher average total carbonyl concentrations in winter than in spring, which could be explained by less rainfall during winter (Table 2) leading to reduced removal of carbonyls by wet scavenging in winter.

3.3. Correlation between carbonyls and meteorological parameters

Pearson's correlation analysis was used to test the correlation between carbonyls and meteorological parameters (Supplementary Materials: Table S3–5). A very strong positive correlation (r > 0.9) is observed between formaldehyde/acetaldehyde and total carbonyl compounds at all locations. Several strongly positive correlations (r > 0.7) and moderately positive correlations (r > 0.5) are observed at all sampling locations. The data can be found in

the Supplementary Materials: Table S3–5. The strong positive correlation between formaldehyde and acetaldehyde implies that the two compounds possibly share similar sources. Stronger positive correlations were observed at TC and YL compared to HT. The TC and YL station are located at urban area, whereas the HT station is at rural area. Past studies showed carbonyls concentrations due to industrial emissions were identified at Tsuen Wan (22^o 22' 18.0"N, 114^o 6' 52.0"E) and Kwai Chung (22^o 21' 26.0"N, 114^o 7' 47.0"E) monitoring stations located in industrial areas (Ho et al., 2002b; Ho et al., 2006) that are remote from the sampling stations in this study. Even stronger positive correlations were identified at TC compared to YL. The underlying reason may be that TC is located downwind from YL, which would favor high carbonyl loading under northeast monsoon conditions. Past studies suggested that a convergence zone can form in the TC area (Fung et al., 2005), which could trap carbonyls being transported by different wind systems from other locations (e.g., sea breezes, synoptic winds, and local circulation). All the above conditions could enhance associations between carbonyl compounds. Carbonyls with carbon numbers higher than formaldehyde show low correlations among one another at HT. This suggests that carbonyls heavier than formaldehyde originate from mixed sources.

Anderson et al. (1996) showed that the most important daytime sinks for both formaldehyde and acetaldehyde are photolysis and reaction with hydroxyl radical. Anderson et al. (1996) also showed that formaldehyde would be to be destroyed faster than acetaldehyde in all seasons. The average concentrations of carbon monoxide and ozone in the sampling locations can be found in Supplementary Materials: Table S1. CO is regarded as being formed from primary emissions (incomplete combustion of vehicle engines), whereas O_3 is generated from photochemical reaction in the tropical atmosphere (Cheng et al., 2014). The concentrations of CO in TC and YL (both urban) are ~2 times higher than HT (rural). The concentration of O_3 in HT is at least ~1.7 times higher than TC and YL, all consistent with the location

characteristics. Previous studies showed that CO at the HT station originated mainly from coastal regions in southern China and from eastern China, and O_3 was influenced by regional transport of O_3 precursors originating in eastern China because of strong continental outflow and regional impacts under a backward Lagrangian particle dispersion model (Ding et al., 2013). Another study suggested, using back trajectory analysis, that O_3 precursors from the eastern coast of China coupled with long-range transport could increase the total ozone in urban areas of Hong Kong (Wang et al., 2009). Such conditions coupled with local CO and O_3 concentrations, together with different tropospheric lifetime of CO and O_3 (Novelli et al., 1998; Stevenson et al., 1999) could possibly affect the overall outcome of the source apportionment analysis.

Formaldehyde (except for TC), acetaldehyde, benzaldehyde, and total carbonyls show significant positive correlations with O_3 and CO, but significant negative correlations with relative humidity at all locations. This suggests the species could come from both of the above-mentioned sources and are associated with the relative humidity, albeit in a negative manner. Relative humidity is negatively correlated with the carbonyls could be due to the species are highly water soluble. Acetaldehyde shows no significant correlations with temperature at TC and YL, implying that the acetaldehyde generated from photochemical reaction at these locations is independent of temperature. Most of the carbonyl species show low and insignificant correlations with wind speed and ultra-violet solar radiation in all locations (except C1 and C2 against UV at TC). The low-to-fair correlation coefficients (Supplementary Materials: Table S3-5) could be due to considerable meteorological variability during the two-year campaign.

3.4. Sources apportionment of formaldehyde

In order to identify the most suitable model for the time series data, different evaluation approaches were performed and can be found in Supplementary Materials: Table S6-7. Statistical tests were performed to determine the mathematical transformations in order to produce the best correlations. The results (Supplementary Materials: Table S6-7) indicate the transformations led to minimal improvement to the model fit, and hence the original data were chosen for the analysis. Hence, Table 3 shows linear regression coefficients, concentration contributions, and relative source contributions of HCHO (>136 sampling days) after consideration of different conditions. Figure 2 shows the relative percentage contributions for the apportionment analysis. The statistical reliability criteria show a significant linear regression (R > 0.4), and significance values confirm that the linear relationships in Eq. (3)–(5) are statistically reliable (Li et al., 2010). The correlation coefficients are low, reflecting large day-to-day variability in the concentration data, possibility due to large meteorological variability. However, the regression analysis was performed solely to determine the means, to investigate statistical inferences about the relationships between concentrations and locations, not to explain large portions of the variance. The contribution from primary sources at HT (~13%) was calculated and compared to the urban areas of TC (~21%) and YL (~40%). The result is consistent with the trend of the total carbonyl concentrations (HT < TC < YL), and both results show similarities with the geographic characteristics of the sampling locations. Location HT is far removed from any direct vehicular emissions compared to TC and YL. Vehicular emissions are an important anthropogenic source of airborne carbonyls in urban areas (Ho et al., 2012). The contribution at YL is comparable to Mexico City (~42%) (Garcia et al., 2006) and a similar regression analysis using CO as a surrogate for identifying primary HCHO (~39%) from vehicle emissions (Rappenglück et al., 2010). The highest contribution from secondary sources occurs at HT (~53%), compared to YL (~36%) and TC (~31%). This suggests more intense

412 photochemical activity, i.e., photochemical oxidation of biogenic VOCs, in rural areas (HT)
413 than in urban areas (YL and TC). However, the contribution from secondary sources (in μg
414 m^{-3}) is (in ascending order): HT < TC < YL. Table 3 shows that the background and primary
415 contributions at HT are ~1.7–4.1 times lower than the secondary contributions. The rather
416 high contribution from secondary sources at HT could be due to relatively low background
417 and primary contributions, as HT shows the lowest formaldehyde concentrations attributable
418 to secondary sources when compared to TC and YL. The result at HT is comparable with the
419 results reported by Friedfeld et al. (2002) for Houston (63%) in 2000. Guven and Olaguer
420 (2011) showed that ~36% HCHO formed by secondary processes came from VOC
421 decomposition and ~24% could be apportioned to biogenic isoprene-related emissions. The
422 combined secondary sources accounted for a ~60% contribution, which is close to HT
423 (~53%). The secondary sources at HT could be potentially due to these two aforementioned
424 sources. Using peroxyacetic nitric anhydride (PAN) as a representative compound,
425 Rappenglück et al. (2010) found that ~24% of secondary HCHO formed photochemically at
426 the Moody Tower site close to downtown Houston. This finding is similar to those for the
427 urban areas of YL and TC, where similar secondary source contributions could be explained
428 by a similar intensity in photochemical activity. The relative background contribution at YL
429 (~24%) is lowest compared to HT (~34%) and TC (~48%). The TC location is situated in a
430 valley and governed by complex airflow patterns due to complicated interactions of thermally
431 induced circulations (e.g., sea–land breezes, mountain–valley winds, drainage flows, and
432 mechanically induced circulations) (Liu and Chan, 2002). Under weak synoptic conditions,
433 local effects dominate and favor buildup of formaldehyde concentrations (Liu and Chan,
434 2002). Such a condition could be the reason for the high TC background contribution. Figure
435 3 shows seasonal variations in the relative contributions from primary, secondary, and
436 background sources of formaldehyde. Further information can be found in the Supplementary

Materials: Table S8. All stations recorded the largest contributions from primary sources during winter, suggesting that direct emissions rather than photochemically induced emissions dominate at low temperatures. Autumn shows the largest contributions from secondary sources at all locations, was characterized by increasing average temperatures (winter: 16.7°C; autumn: 25.1°C), along with reduced average relative humidity (winter: 76.1%; autumn: 75.1%) and longer average sunshine hours (winter: 4.9 h; autumn: 6.5 h), in the absence of optimum average temperatures and UV solar radiation (summer: 28.5°C/953 W m^{-2}; autumn: 25.1°C/851 W m^{-2}). This particular set of conditions could favor secondary sources of HCHO contribution. The highest background HCHO concentrations occur in the summer at all stations. This could be caused by prevailing southerly or southeasterly winds, which transport clean marine air masses from the South China Sea or the Northwest Pacific Ocean, diluting the primary and secondary HCHO loadings.

4. Conclusions

Characteristics of carbonyl and formaldehyde sources were investigated. Formaldehyde and acetaldehyde are the two most abundant carbonyls. Acetone was not analyzed due to negative biases and poor collection efficiency of acetone in the method (U.S. EPA Method TO-11A). A strong positive correlation between formaldehyde and acetaldehyde implies that the two compounds possibly share similar sources. Contributions from primary HCHO sources at HT (~13%), TC (~21%), and YL (~40%) are consistent with average total carbonyl concentration trends (HT < TC < YL). Unique geographic features at TC, coupled with meteorological conditions, seem to favor accumulation of formaldehyde. Primary sources are largest in winter, suggesting that direct rather than photochemically induced emissions dominate at low temperatures. However, the overall source apportionment results contain significant uncertainties such as insufficient knowledge of HCHO and precursor emissions at the

462 sampling stations. Further limitations of this study may arise from transport and chemical
463 transformation of HCHO because of contributions from different sources. Additional studies
464 should focus on quantifying and harmonizing these uncertainties to improve future
465 apportionment analyses.

466

467 **Disclaimer**

468 The opinions expressed in this paper are those of the author and do not necessarily reflect the
469 views or policies of the Government of the Hong Kong Special Administrative Region, nor
470 does mention of trade names or commercial products constitute an endorsement or
471 recommendation of their use.

472

473 **Acknowledgments**

474 This study is supported by a grant from the Research Grants Council of the Hong Kong
475 Special Administrative Region of China (Project No. CUHK 412612). The author would like
476 to thank Xiao-Cui Chen for her assistance in the laboratory.

477

478 **References**

479 Anderson, L.G., Lanning, J.A., Barrell, R., Miyagishima, J., Jones, R.H., Wolfe, P., 1996.
480 Sources and sinks of formaldehyde and acetaldehyde: An analysis of Denver's ambient
481 concentration data. Atmospheric Environment 30, 2113-2123.
482 Atkinson, R., 2000. Atmospheric chemistry of VOCs and NOx. Atmospheric Environment
483 34, 2063-2101.
484 Carlier, P., Hannachi, H., Mouvier, G., 1986. The chemistry of carbonyl compounds in the
485 atmosphere—a review. Atmospheric Environment 20, 2079-2099.
486 Census and Statistics Department, The Government of the Hong Kong Special
487 Administrative Region, 2011. Hong Kong 2011 Population Census - Summary Results.

Cheng, Y., Lee, S., Huang, Y., Ho, K., Ho, S., Yau, P., Louie, P., Zhang, R., 2014. Diurnal and seasonal trends of carbonyl compounds in roadside, urban, and suburban environment of Hong Kong. Atmospheric Environment 89, 43-51.

Dean, J.A., 1999. Lange's Handbook of Chemistry. McGraw-Hill, Inc. New York.

Dee, D., Uppala, S., Simmons, A., Berrisford, P., Poli, P., Kobayashi, S., Andrae, U., Balmaseda, M., Balsamo, G., Bauer, P., 2012. The ERA-interim reanalysis: configuration and performance of the data assimilation system, data available at: http://data-portal.ecmwf.int/data/d/interimmoda/levtype= sfc/, last access 4, 553-597.

De Smedt, I., Müller, J.-F., Stavrakou, T., van der A, R., Eskes, H., Van Roozendael, M., 2008. Twelve years of global observations of formaldehyde in the troposphere using GOME and SCIAMACHY sensors. Atmospheric Chemistry and Physics 8, 4947-4963.

DeMore, W.B., Sander, S.P., Golden, D.M., Hampson, R.F., Kuzylo, M.J., Howard, C.J., Ravishankara, A.R., Kolb, C., Molina, M.J., 1992. Chemical kinetics and photochemical data for use in stratospheric modeling: Evaluation Number 10.

Ding, A., Wang, T., Fu, C., 2013. Transport characteristics and origins of carbon monoxide and ozone in Hong Kong, South China. Journal of Geophysical Research: Atmospheres 118, 9475-9488.

Feng, Y., Wen, S., Chen, Y., Wang, X., Lü, H., Bi, X., Sheng, G., Fu, J., 2005. Ambient levels of carbonyl compounds and their sources in Guangzhou, China. Atmospheric Environment 39, 1789-1800.

Feng, Y., Wen, S., Wang, X., Sheng, G., He, Q., Tang, J., Fu, J., 2004. Indoor and outdoor carbonyl compounds in the hotel ballrooms in Guangzhou, China. Atmospheric Environment 38, 103-112.

Friedfeld, S., Fraser, M., Ensor, K., Tribble, S., Rehle, D., Leleux, D., Tittel, F., 2002. Statistical analysis of primary and secondary atmospheric formaldehyde. Atmospheric Environment 36, 4767-4775.

Fung, J., Lau, A., Lam, J., Yuan, Z., 2005. Observational and modeling analysis of a severe air pollution episode in western Hong Kong. Journal of Geophysical Research: Atmospheres (1984-2012) 110.

Garcia, A., Volkamer, R., Molina, L., Molina, M., Samuelson, J., Mellqvist, J., Galle, B., Herndon, S., Kolb, C., 2006. Separation of emitted and photochemical formaldehyde in Mexico City using a statistical analysis and a new pair of gas-phase tracers. Atmospheric Chemistry and Physics 6, 4545-4557.

Grosjean, D., 1991. Ambient levels of formaldehyde, acetaldehyde and formic acid in southern California: results of a one-year baseline study. Environmental science & technology 25, 710-715.

Grosjean, D., Grosjean, E., Moreira, L.F., 2002. Speciated ambient carbonyls in Rio de Janeiro, Brazil. Environmental Science and Technology 36, 1389-1395.

Grosjean, E., Grosjean, D., Fraser, M.P., Cass, G.R., 1996. Air quality model evaluation data for organics. 2. C1-C14 carbonyls in Los Angeles air. Environmental Science and Technology 30, 2687-2703.

Guo, S.-J., Chen, M., He, X.-L., Yang, W.-W., Tan, J.-H., 2014. Seasonal and Diurnal Characteristics of Carbonyls in Urban Air in Qinzhou, China. Aerosol and Air Quality Research 14, 1653-1664.

Guven, B.B., Olaguer, E.P., 2011. Ambient formaldehyde source attribution in Houston during TexAQS II and TRAMP. Atmospheric Environment 45, 4272-4280.

Ho, K., Ho, S.S.H., Cheng, Y., Lee, S., Yu, J.Z., 2007. Real-world emission factors of fifteen carbonyl compounds measured in a Hong Kong tunnel. Atmospheric Environment 41, 1747-1758.

Ho, K., Lee, S., Tsai, W., 2006. Carbonyl compounds in the roadside environment of Hong Kong. Journal of hazardous materials 133, 24-29.

Ho, K., Lee, S., Chiu, G.M., 2002a. Characterization of selected volatile organic compounds, polycyclic aromatic hydrocarbons and carbonyl compounds at a roadside monitoring station. Atmospheric Environment 36, 57-65.

Ho, K., Lee, S., Louie, P.K., Zou, S., 2002b. Seasonal variation of carbonyl compound concentrations in urban area of Hong Kong. Atmospheric Environment 36, 1259-1265.

Ho, S.S.H., Chow, J.C., Watson, J.G., Ip, H.S.S., Ho, K.F., Dai, W.T., Cao, J., 2014. Biases in ketone measurements using DNPH-coated solid sorbent cartridges. Analytical Methods 6, 967-974.

Ho, S.S.H., Ho, K.F., Lee, S.C., Cheng, Y., Yu, J.Z., Lam, K.M., Feng, N.S.Y., Huang, Y., 2012. Carbonyl emissions from vehicular exhausts sources in Hong Kong. Journal of the Air & Waste Management Association 62, 221-234.

Ho, S.S.H., Ho, K.F., Liu, W.D., Lee, S.C., Dai, W.T., Cao, J.J., Ip, H.S.S., 2011. Unsuitability of using the DNPH-coated solid sorbent cartridge for determination of airborne unsaturated carbonyls. Atmospheric Environment 45, 261-265.

553 Hong Kong Transportation Department, The Government of the Hong Kong Special
554 Administrative Region, 2013. Monthly Traffic and Transport Digest.
555 IARC, 2004. IARC monographs on the evaluation of carcinogenic risks to humans. IARC.
556 IARC, 2006. IARC monographs on the evaluation of carcinogenic risks to humans-
557 formaldehydes, 2-butoxyethanol and 1-tert-Butoxypropan-2-ol. IARC.
558 Jaffe, L.S., 1968. Ambient carbon monoxide and its fate in the atmosphere. Journal of the Air
559 Pollution Control Association 18, 534-540.

560 Kean, A.J., Grosjean, E., Grosjean, D., Harley, R.A., 2001. On-road measurement of
561 carbonyls in California light-duty vehicle emissions. Environmental Science and
562 Technology 35, 4198-4204.
563 Lee, M., Heikes, B.G., Jacob, D.J., Sachse, G., Anderson, B., 1997. Hydrogen peroxide,
564 organic hydroperoxide, and formaldehyde as primary pollutants from biomass burning.
565 Journal of Geophysical Research: Atmospheres (1984–2012) 102, 1301-1309.
566 Li, Y., Shao, M., Lu, S., Chang, C.-C., Dasgupta, P.K., 2010. Variations and sources of
567 ambient formaldehyde for the 2008 Beijing Olympic games. Atmospheric Environment
568 44, 2632-2639.
569 Liu, H., Chan, J.C., 2002. Boundary layer dynamics associated with a severe air-pollution
570 episode in Hong Kong. Atmospheric Environment 36, 2013-2025.
571 Moussa, S.G., El-Fadel, M., Saliba, N.A., 2006. Seasonal, diurnal and nocturnal behaviors of
572 lower carbonyl compounds in the urban environment of Beirut, Lebanon. Atmospheric
573 Environment 40, 2459-2468.
574 Novelli, P., Masarie, K., Lang, P., 1998. Distributions and recent changes of carbon monoxide
575 in the lower troposphere. Journal of Geophysical Research: Atmospheres 103, 19015-
576 19033.

577 Parrish, D., Ryerson, T., Mellqvist, J., Johansson, J., Fried, A., Richter, D., Walega, J.,
578 Washenfelder, R., De Gouw, J., Peischl, J., 2012. Primary and secondary sources of
579 formaldehyde in urban atmospheres: Houston Texas region. Atmospheric Chemistry and
580 Physics 12, 3273-3288.
581 Perry, R., Gee, I.L., 1995. Vehicle emissions in relation to fuel composition. Science of the
582 Total Environment 169, 149-156.
583 Rappenglück, B., Dasgupta, P., Leuchner, M., Li, Q., Luke, W., 2010. Formaldehyde and its
584 relation to CO, PAN, and SO 2 in the Houston-Galveston airshed. Atmospheric
585 Chemistry and Physics 10, 2413-2424.

Schulte-Ladbeck, R., Lindahl, R., Levin, J.O., Karst, U., 2001. Characterization of chemical interferences in the determination of unsaturated aldehydes using aromatic hydrazine reagents and liquid chromatography. Journal of Environmental Monitoring 3, 306-310.

Shepson, P., Hastie, D., Schiff, H., Polizzi, M., Bottenheim, J., Anlauf, K., Mackay, G., Karecki, D., 1991. Atmospheric concentrations and temporal variations of C1-C3 carbonyl compounds at two rural sites in central Ontario. Atmospheric Environment. Part A. General Topics 25, 2001-2015.

Social Welfare Department, The Government of the Hong Kong Special Administrative Region, 2013. Population Profile of Yuen Long District.

Spaulding, R.S., Frazey, P., Rao, X., Charles, M.J., 1999. Measurement of hydroxy carbonyls and other carbonyls in ambient air using pentafluorobenzyl alcohol as a chemical ionization reagent. Analytical Chemistry 71, 3420-3427.

Stevenson, D., Dentener, F., Schultz, M., Ellingsen, K., Van Noije, T., Wild, O., Zeng, G., Amann, M., Atherton, C., Bell, N., 2006. Multimodel ensemble simulations of present-day and near-future tropospheric ozone. Journal of Geophysical Research: Atmospheres 111, D08301.

Streets, D., Yarber, K., Woo, J.H., Carmichael, G., 2003. Biomass burning in Asia: Annual and seasonal estimates and atmospheric emissions. Global Biogeochemical Cycles 17.

Stull, R.B., 2012. An introduction to boundary layer meteorology. Springer Science & Business Media.

USEPA, Compendium of Methods for the Determination of Toxic Organic Compounds in Ambient Air Second Edition: Compendium Method TO-11A Determination of Formaldehyde in Ambient Air Using Adsorbent Cartridge Followed by High Performance Liquid Chromatography (HPLC) [Active Sampling Methodology], (1999).

Villanueva, F., Tapia, A., Notario, A., Albaladejo, J., Martínez, E., 2014. Ambient levels and temporal trends of VOCs, including carbonyl compounds, and ozone at Cabañeros National Park border, Spain. Atmospheric Environment 85, 256-265.

Wang, T., Wei, X., Ding, A., Poon, S.C., Lam, K., Li, Y., Chan, L., Anson, M., 2009. Increasing surface ozone concentrations in the background atmosphere of Southern China, 1994-2007. Atmospheric Chemistry and Physics 9, 6217-6227.

Watson, J.G., Lioy, P.J., Mueller, P.K., 1995. The measurement process: precision, accuracy, and validity. Air Sampling Instruments for Evaluation of Atmospheric Contaminants, 8th ed. American Conference of Governmental Industrial Hygienists, Cincinnati, OH.

Wert, B., Trainer, M., Fried, A., Ryerson, T., Henry, B., Potter, W., Angevine, W., Atlas, E., Donnelly, S., Fehsenfeld, F., 2003. Signatures of terminal alkene oxidation in airborne formaldehyde measurements during TexAQS 2000. Journal of Geophysical Research: Atmospheres (1984–2012) 108.

WHO, 2000. Air Quality Guidelines for Europe, 2nd edition, 2000. World Health Organization, Denmark, pp. 87-91.

Yang, D., Li, C., Lau, A.K.H., Li, Y., 2013. Long-term measurement of daytime atmospheric mixing layer height over Hong Kong. Journal of Geophysical Research: Atmospheres 118, 2422-2433.

Yokelson, R.J., Goode, J.G., Ward, D.E., Susott, R.A., Babbitt, R.E., Wade, D.D., Bertschi, I., Griffith, D.W., Hao, W.M., 1999. Emissions of formaldehyde, acetic acid, methanol, and other trace gases from biomass fires in North Carolina measured by airborne Fourier transform infrared spectroscopy. Journal of Geophysical Research: Atmospheres (1984–2012) 104, 30109-30125.

Figure Legends

List of Tables

List of Figures

643 Figure 2 Relative HCHO contributions from primary, secondary, and background
644 sources (percent)

645 Figure 3 Seasonal variations of relative contributions from primary, secondary, and
646 background HCHO sources (percent)

Table
Click here to download Table: Tables(Carbonyls)_AE_Review.docx

1 Table 1 Descriptive analysis and relative abundances of carbonyl concentrations

Sampling Location		C1	C2	nC3	MEK	iso+nC4	benz	iso-C5	nC5	o-tol	m-tol	p-tol	C6	2,5-DB	Total Carbonyls
		μg/m^3													
Hok Tsui (HT)	2012														
	Winter	2.4±0.6	1.4±0.4	0.2±0.1	0.2±0.1	0.1±0.1	0.2±0.1	0.1±0.1	0.1±0.1	B.D.	B.D.[b]	B.D.	0.1±0.1	B.D.	4.8±1.2
	Spring	2.2±0.6	0.9±0.5	0.3±0.3	0.1±0.1	0.2±0.1	0.1±0.1	0.1±0.1	0.1±0.1	B.D.	0.03±0.01	B.D.	0.1±0.1	B.D.	4.1±1.3
	Summer	2.1±1.4	0.8±0.7	0.1±0.1	0.1±0.1	0.1±0.1	0.1±0.1	0.1±0.1	0.1±0.1	B.D.	B.D.	B.D.	0.1±0.1	B.D.	3.6±2.4
	Autumn	2.9±1.5	1.2±0.6	0.1±0.1	0.1±0.1	0.1±0.1	0.1±0.1	0.1±0.1	0.1±0.1	B.D.	B.D.	B.D.	0.1±0.1	B.D.	4.8±2.3
	Overall	2.4±0.5	1.1±0.1	0.1±0.1	0.2±0.1	0.1±0.1	0.1±0.1	0.1±0.1	0.1±0.1	B.D.	B.D.	B.D.	0.1±0.1	B.D.	4.3±0.6
	S/W[a]	0.9	0.6	0.5	0.5	0.1	0.5	0.1	0.1	N.A.	N.A.[c]	N.A.	0.1	N.A.	0.8
	2013														
	Winter	2.6±1.1	1.2±0.5	0.1±0.1	0.2±0.1	0.1±0.1	0.1±0.1	0.1±0.1	0.1±0.1	B.D.	B.D.	B.D.	0.1±0.1	B.D.	4.6±1.9
	Spring	1.7±0.2	0.9±0.1	0.1±0.1	0.1±0.1	0.1±0.1	0.1±0.1	0.1±0.1	0.1±0.1	B.D.	B.D.	B.D.	0.1±0.1	B.D.	3.3±0.5
	Summer	1.7±0.4	0.6±0.2	0.1±0.1	0.03±0.01	0.1±0.1	0.1±0.1	0.2±0.1	0.1±0.1	B.D.	B.D.	B.D.	0.1±0.1	B.D.	3.0±0.7
	Autumn	4.1±2.2	1.5±0.9	0.1±0.1	0.1±0.1	0.1±0.1	0.2±0.1	0.1±0.1	0.1±0.1	B.D.	B.D.	B.D.	0.1±0.1	B.D.	6.4±3.1
	Overall	2.5±1.0	1.0±0.3	0.1±0.1	0.1±0.1	0.1±0.1	0.1±0.1	0.1±0.1	0.1±0.1	B.D.	B.D.	B.D.	0.1±0.1	B.D.	4.2±1.2
	S/W	0.7	0.5	0.1	0.2	0.1	0.1	2	0.1	N.A.	N.A.	N.A.	0.1	N.A.	0.7
Tung Chung (TC)	2012														
	Winter	4.3±1.4	2.3±0.8	0.4±0.2	0.7±0.3	0.3±0.1	0.2±0.1	0.3±0.2	0.1±0.1	B.D.	0.1±0.1	B.D.	0.2±0.1	B.D.	8.9±2.5
	Spring	4.5±1.0	1.8±0.7	0.3±0.2	0.3±0.2	0.3±0.1	0.1±0.1	0.3±0.2	0.1±0.1	B.D.	0.1±0.1	B.D.	0.3±0.1	B.D.	8.1±2.0
	Summer	4.7±2.4	2.5±1.4	0.3±0.2	0.2±0.2	0.3±0.3	0.1±0.2	0.4±0.2	0.1±0.1	B.D.	B.D.	B.D.	0.5±0.5	B.D.	9.1±4.9
	Autumn	4.7±2.8	2.2±1.6	0.3±0.2	0.4±0.4	0.2±0.2	0.2±0.2	0.5±0.7	0.1±0.1	B.D.	B.D.	B.D.	0.1±0.1	B.D.	8.7±5.7
	Overall	4.6±0.9	2.2±0.4	0.3±0.1	0.4±0.1	0.3±0.1	0.2±0.1	0.4±0.3	0.1±0.1	B.D.	B.D.	B.D.	0.3±0.2	B.D.	8.8±1.8
	S/W	1.1	1.1	0.8	0.3	1	0.5	1.3	1	N.A.	N.A.	N.A.	2.5	N.A.	1
	2013														
	Winter	4.0±1.3	2.3±1.0	0.3±0.2	0.4±0.4	0.3±0.1	0.3±0.2	0.4±0.3	0.1±0.1	B.D.	B.D.	B.D.	0.2±0.1	B.D.	8.3±3.3
	Spring	3.3±0.7	1.8±0.4	0.2±0.1	0.3±0.1	0.3±0.1	0.2±0.1	0.2±0.1	0.1±0.1	B.D.	0.1±0.1	B.D.	0.2±0.1	B.D.	6.7±1.4
	Summer	4.2±0.8	2.0±0.6	0.3±0.1	0.1±0.1	0.2±0.1	0.1±0.1	0.4±0.1	0.2±0.1	B.D.	0.03±0.01	B.D.	1.2±0.4	B.D.	8.7±1.6
	Autumn	6.7±2.4	3.3±1.3	0.5±0.2	0.2±0.1	0.4±0.1	0.3±0.2	0.5±0.3	0.1±0.1	B.D.	B.D.	B.D.	0.3±0.1	B.D.	12.3±4.4
	Overall	4.6±0.8	2.3±0.4	0.3±0.1	0.3±0.2	0.3±0.1	0.2±0.1	0.4±0.1	0.1±0.1	B.D.	B.D.	B.D.	0.5±0.1	B.D.	9.0±1.4
	S/W	1.1	0.9	1	0.3	0.7	0.3	1	2	N.A.	N.A.	N.A.	6	N.A.	1
Yuen	2012														

Long (YL)	Winter	4.6±1.0	2.7±0.5	0.7±0.5	0.9±0.3	0.3±0.1	0.4±0.1	0.6±0.2	0.2±0.1	B.D.	0.2±0.1	B.D.	0.4±0.1	B.D.	11.0±1.5
	Spring	4.3±1.2	2.1±0.9	0.3±0.1	0.4±0.2	0.3±0.1	0.3±0.2	0.4±0.2	0.3±0.1	0.1±0.1	0.1±0.1	B.D.	0.4±0.2	B.D.	9.0±2.7
	Summer	3.8±2.3	2.1±1.3	0.4±0.2	0.2±0.1	0.2±0.1	0.2±0.2	0.4±0.4	0.1±0.1	B.D.	0.03±0.01	B.D.	0.3±0.1	B.D.	7.7±4.1
	Autumn	4.8±2.3	2.9±1.1	0.5±0.3	0.6±0.6	0.4±0.2	0.3±0.3	0.8±0.7	0.1±0.1	B.D.	B.D.	B.D.	0.3±0.2	B.D.	10.7±4.4
	Overall	4.3±0.7	2.4±0.3	0.5±0.1	0.5±0.2	0.3±0.1	0.3±0.1	0.6±0.3	0.2±0.1	B.D.	B.D.	B.D.	0.3±0.1	B.D.	9.4±1.3
	S/W	0.8	0.8	0.6	0.2	0.7	0.5	0.7	0.5	N.A.	0.2	N.A.	0.8	N.A.	0.7
	2013														
	Winter	5.6±2.0	3.4±1.5	0.5±0.3	0.9±1.1	0.4±0.2	0.3±0.2	0.6±0.4	0.1±0.1	B.D.	B.D.	B.D.	0.5±0.2	B.D.	12.3±5.1
	Spring	3.5±0.8	2.1±0.6	0.3±0.1	0.5±0.2	0.3±0.1	0.3±0.1	0.4±0.1	0.2±0.1	0.04±0.02	0.1±0.1	B.D.	0.3±0.1	B.D.	8.0±2.1
	Summer	3.4±0.7	1.7±0.5	0.3±0.1	0.1±0.1	0.1±0.1	0.1±0.1	0.9±0.5	0.1±0.1	B.D.	0.02±0.01	0.02±0.01	0.4±0.1	B.D.	7.1±1.0
	Autumn	8.3±2.7	4.1±1.5	0.6±0.2	0.3±0.1	0.4±0.2	0.4±0.2	0.5±0.2	0.1±0.1	B.D.	B.D.	B.D.	0.5±0.1	B.D.	15.2±4.8
	Overall	5.2±1.0	2.8±0.6	0.4±0.1	0.5±0.5	0.3±0.1	0.3±0.1	0.6±0.2	0.1±0.1	B.D.	B.D	B.D.	0.4±0.1	B.D.	10.6±2.0
	S/W	0.6	0.5	0.6	0.1	0.3	0.3	1.5	1	N.A.	N.A.	N.A.	0.8	N.A.	0.6

[a]S/W indicates summer to winter ratio

[b]B.D. indicates below detection limit

[c]N.A. indicates not available

Table 2 Average meteorological parameters during the sampling period

		Pressure (hPa)	Temperature (°C)	Relative Humidity (%)	Cloud (%)	Rainfall (mm)	Reduced Visibility (hour)	Sunshine Hours	UV Solar Radiation (W/m^2)	Wind Speed (m/s)	Wind Direction (°)
2012	Winter	1018.2±3.7	16.2±2.8	81.4±9.0	78.9±2.9	4.0±3.7	4.7±6.3	3.9±3.4	489.9±285.9	7.4±2.5	45.6±20.6
	Spring	1011.5±4.5	23.3±4.1	84.8±9.0	77.9±4.1	13.8±19.2	1.3±2.5	4.3±3.3	765.0±401.5	6.4±2.4	103.3±71.7
	Summer	1003.5±3.3	28.8±1.4	80.6±7.1	73.0±1.2	16.9±25.0	1.0±2.3	5.7±3.5	975.5±386.4	6.1±3.1	178.0±76.2
	Autumn	1013.4±2.8	25.2±2.8	76.8±9.1	66.6±2.8	9.2±21.2	2.0±4.5	6.0±3.4	814.8±380.7	6.7±2.6	76.7±38.7
2013	Winter	1019.5±2.9	17.2±3.0	70.8±2.7	57.3±2.7	8.5±4.4	8.3±8.6	5.8±3.3	728.0±265.7	6.4±2.2	45.1±21.3
	Spring	1012.2±4.5	22.6±3.8	84.0±3.5	75.1±3.5	16.5±33.0	1.9±3.9	3.8±3.5	662.3±389.1	5.7±2.6	109.9±78.8
	Summer	1005.8±3.2	28.2±2.0	83.9±1.5	70.9±1.3	21.3±27.5	0.2±1.3	5.2±3.8	930.1±446.0	6.1±3.1	158.6±71.7
	Autumn	1013.3±5.3	25.0±3.6	73.4±3.3	59.6±3.4	18.0±39.4	2.4±4.8	6.9±3.3	887.6±350.4	7.5±2.8	71.8±43.6

Table 3 Linear regression coefficients, concentrations and relative contributions of primary, secondary, and background sources of HCHO

Sampling Location	b_0 (Background)	b_1 (Secondary)	b_2 (Primary)	R	Sig.
Tung Chung	2.258 (1.234, 3.283)	0.033 (0.022, 0.044)	0.0015 (0.0004, 0.0026)	0.46	0.000
Relative Contributions (%)	48.3±9.4	30.4±13.1	21.3±8.5		
Concentration Contributions (μg/m^3)	2.26	1.58	1.02		
Yuen Long	1.185 (-0.015, 2.385)	0.054 (0.041, 0.068)	0.0028 (0.0014, 0.0041)	0.59	0.000
Relative Contributions (%)	24.0±6.7	36.2±15.8	39.8±12.6		
Concentration Contributions (μg/m^3)	1.19	2.09	2.06		
Hok Tsui	0.867 (0.253, 1.482)	0.019 (0.012, 0.026)	0.0011 (-0.0001, 0.0023)	0.50	0.000
Relative Contributions (%)	34.5±11.3	52.5±11.3	13.0±7.3		
Concentration Contributions (μg/m^3)	0.87	1.52	0.37		

Figure

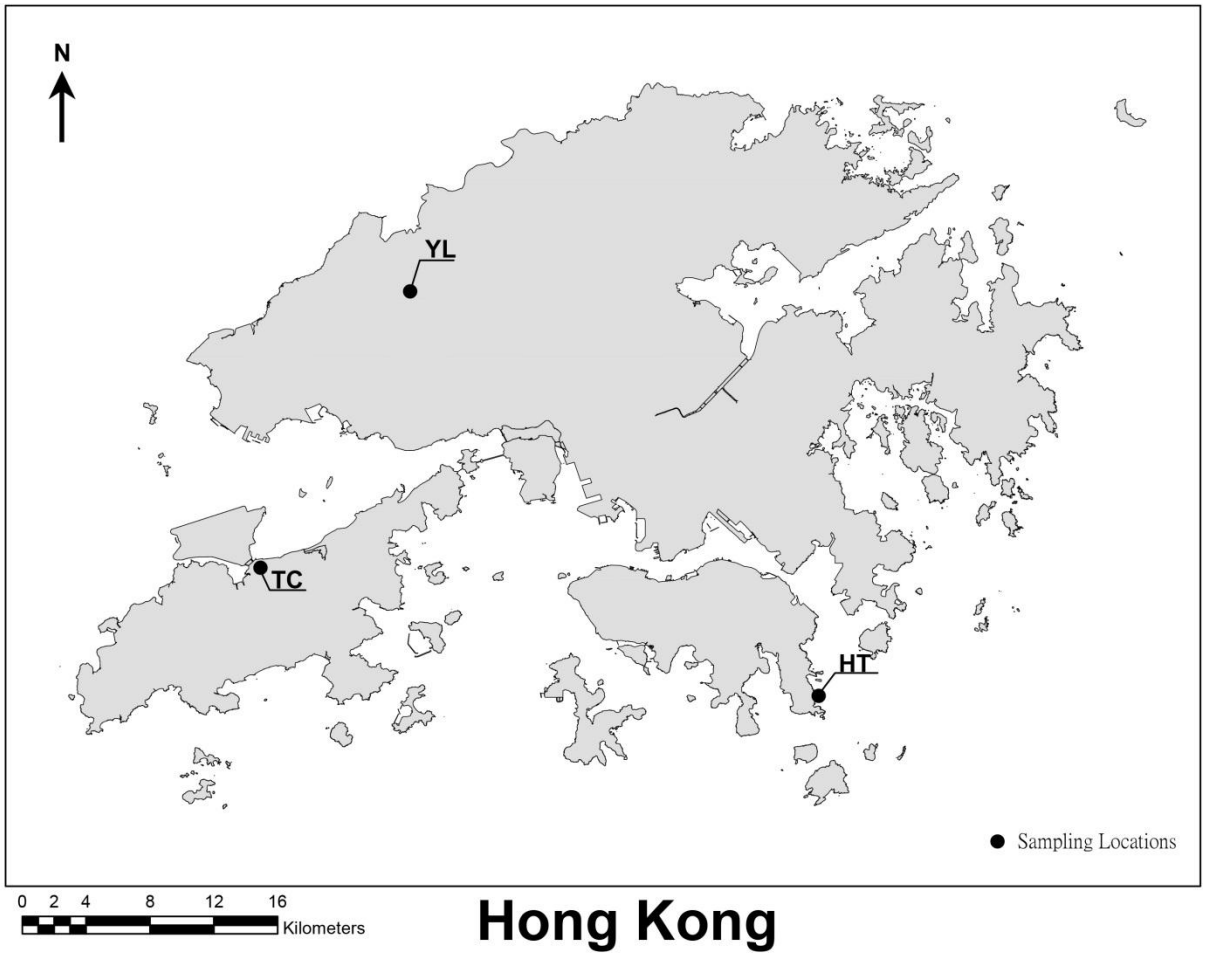

Figure 1 Sampling locations in Hong Kong

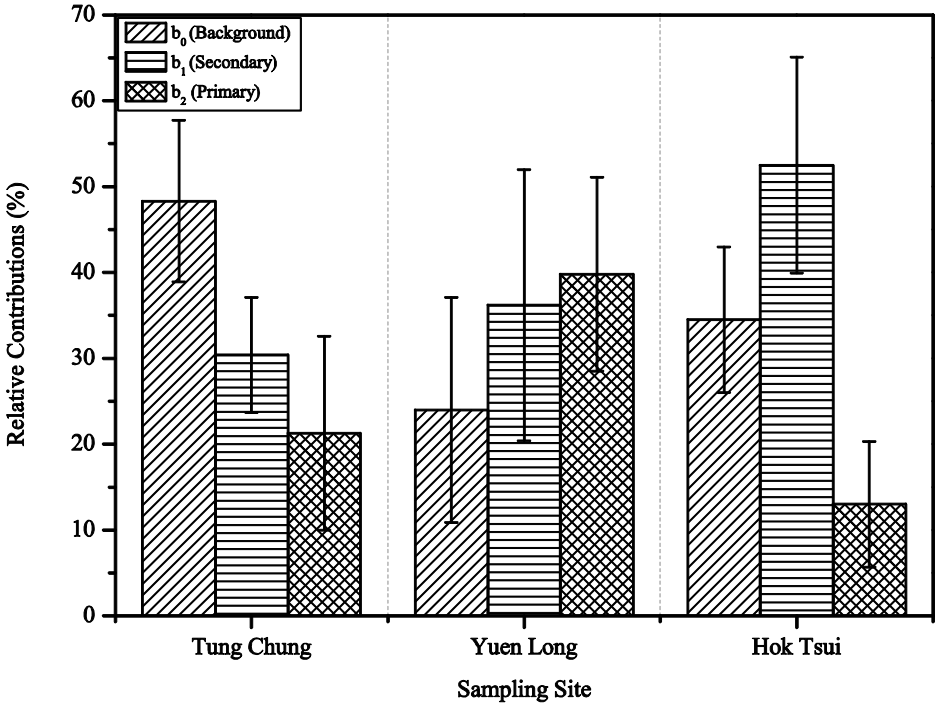

Figure 2 Relative HCHO contributions from primary, secondary, and background sources (percent)

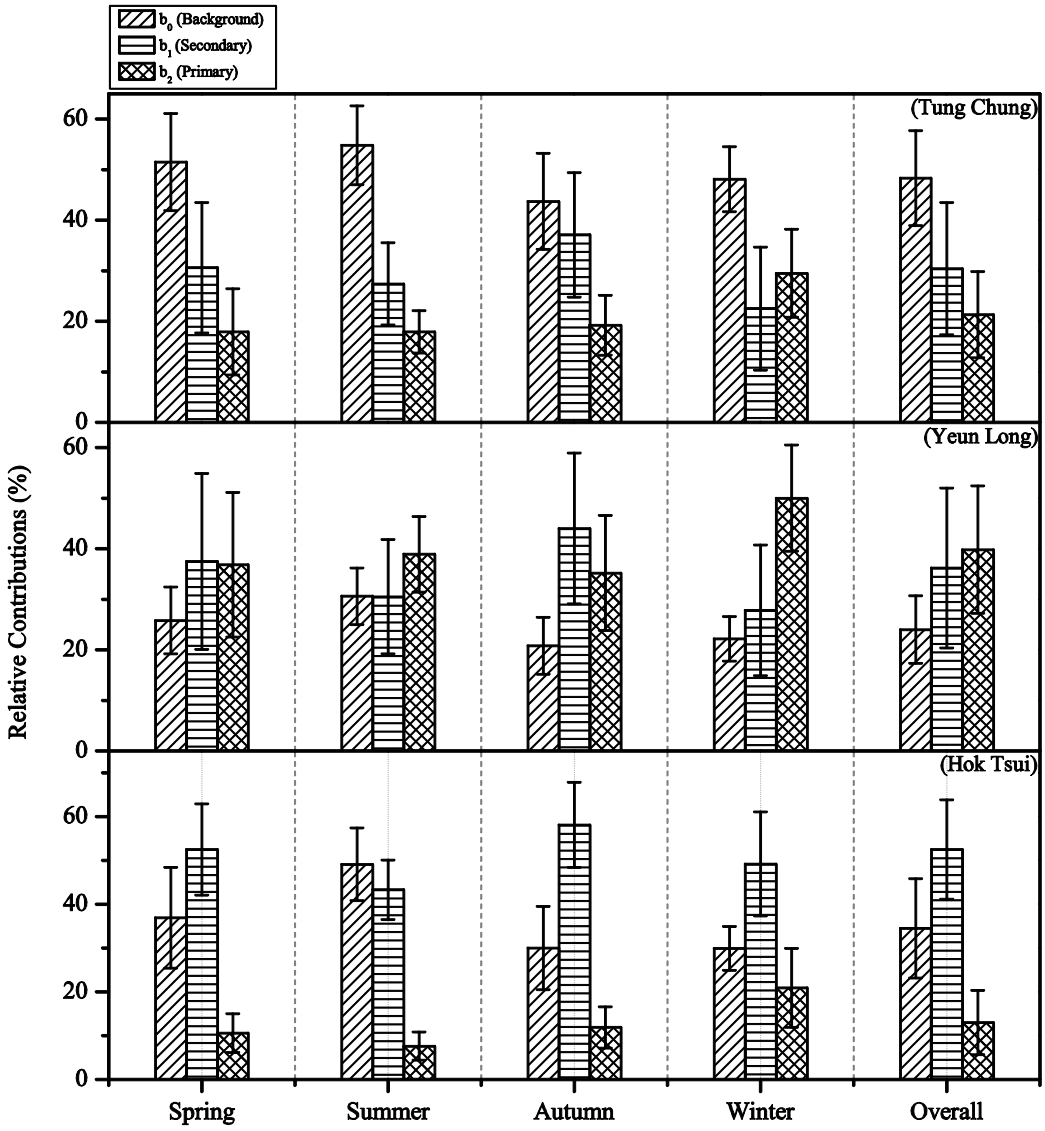

Figure 3 Seasonal variations of relative contributions from primary, secondary, and background HCHO sources (percent)

Supplementary Material

Click here to download Supplementary Material: SupplementaryMaterial(Carbonyls)_AE_2_U.docx